

Soil Moisture Continues Declining in North China over the Regional Warming Slowdown of the Past 20 Years

XIN LI,^{a,b,c} GUOYU REN,^{a,d} QINGLONG YOU,^e SUYAN WANG,^{b,c} AND WEN ZHANG^{b,c}

^a *Department of Atmospheric Science, School of Environmental Studies, China University of Geosciences, Wuhan, China*

^b *Key Laboratory of Meteorological Disaster Monitoring and Early Warning and Risk Management of Characteristic Agriculture in Arid Regions, CMA, Yinchuan, China*

^c *Ningxia Climate Center, CMA, Yinchuan, China*

^d *Laboratory for Climate Studies, National Climate Center, CMA, Beijing, China*

^e *Department of Atmospheric and Oceanic Sciences and Institute of Atmospheric Sciences, Fudan University, Shanghai, China*

(Manuscript received 18 November 2020, in final form 3 September 2021)

ABSTRACT: Soil moisture is an important variable of the climate system and is used to measure dry–wet change in hydroclimate. The warming trend has slowed in China over the past 20 years since 1998, and how the soil moisture changes in this period deserves our attention. With North China as a research region, this study uses the Global Land Data Assimilation System and ground observations to investigate the causes of changes in soil moisture during 1998–2017 versus 1961–97. The results show that 1) annual mean soil moisture experienced an almost continued decrease from the 1960s to 2010s, and no pause in the decrease of soil moisture over the regional warming slowdown of the past 20 years could be detected; 2) with the stabilization or even increase in solar radiation and wind speed as well as the continuous increase of land surface air temperature, the impact of potential evapotranspiration on soil moisture gradually became prominent, and the impact of precipitation decreased, since 1998; 3) the percent contribution of annual potential evapotranspiration to soil moisture variation increased by 26% during 1998–2017 relative to that in 1961–97, and the percent contribution of summer potential evapotranspiration even increased by 45%. Our results will provide insight into the land surface water budget and mechanism involved in drought development in North China.

KEYWORDS: Drought; Precipitation; Moisture/moisture budget; Regional effects; Soil moisture

1. Introduction

Soil moisture is an important variable of the climate system and provides information about surface hydroclimatic processes. Soil moisture directly or indirectly affects the exchange of heat, moisture, and materials between the surface and the atmosphere by changing the soil physical properties such as albedo and soil heat capacity as well as vegetation growth conditions; it also affects local and regional climates, thereby making it an important variable in measuring dry–wet changes (Q. Liu et al. 2011; Orth and Seneviratne 2017). Studies suggested that global warming is accelerating movement of water in the hydrological cycle, which leads to the “dry areas getting drier, wet areas getting wetter” (DGDWGW) paradigm in mid- and high latitudes globally (Liepert and Romanou 2005; Trenberth 2011). Satellite-monitored soil moisture data revealed, however, that, between 1979 and 2013, about 30% of the soil on Earth underwent significant moisture changes, while only 15.12% of the global land soil showed the DGDWGW paradigm (Feng and Zhang 2015). Anthropogenic global warming may exacerbate the reduction in soil moisture in many areas. The growth rate of the water deficit (potential evapotranspiration minus actual evapotranspiration) in the Northern

Hemisphere has increased significantly since 2000 (McCabe and Wolock 2015; Samaniego et al. 2018).

Between 1948 and 2010, the overall level of soil moisture across East Asia showed a decreasing trend, in particular, northeast China, North China, parts of Mongolia, and Russian regions near Lake Baikal showed the most significant decreasing trends, while most of Xinjiang Province and the Qinghai–Tibet Plateau as well as parts of Yunnan Province presented increasing trends in soil moisture, with the decrease of soil moisture taking place in more areas of China than the areas experiencing an increase of soil moisture (Wang et al. 2011; Cheng et al. 2015).

North China (35.25°–42.25°N, 110.25°–129.75°E), most of which is located in the semihumid areas of China, is a region showing sensitive responses of land surface evapotranspiration to rising air temperatures (Jung et al. 2010; Seneviratne et al. 2010; Zhang et al. 2018). The response mechanism of land surface evapotranspiration to climate warming mainly includes two processes: 1) an increase in temperature directly results in an increase in potential evapotranspiration (PET); and 2) the warming-induced evapotranspiration causes a loss of soil moisture, which in turn indirectly inhibits evapotranspiration. The vapor pressure deficit (VPD) is one of key factors controlling evaporative demand, with increasing in VPD possibly reducing soil moisture (Jiao et al. 2021). However, the net radiation reaching the surface and the sensible heat transferred by the wind from local or regional sources are also the primary

Corresponding author: G. Y. Ren, guoyoo@cma.gov.cn

DOI: 10.1175/JHM-D-20-0274.1

© 2021 American Meteorological Society. For information regarding reuse of this content and general copyright information, consult the AMS Copyright Policy (www.ametsoc.org/PUBSReuseLicenses).

Brought to you by LIBRARY OF STATE METEOROLOGICAL | Unauthenticated | Downloaded 11/06/21 08:47 AM UTC

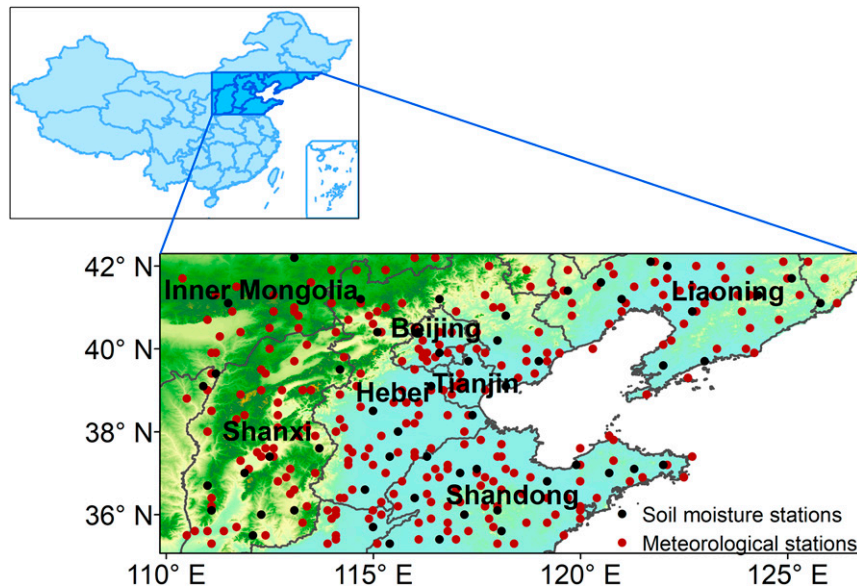


FIG. 1. Study region showing the distribution of meteorological stations and soil moisture stations. An inset maps shows the location of the study area within China.

energy sources of PET (Basso et al. 2021). The increase in potential evapotranspiration not only exacerbates droughts in areas where precipitation has been significantly reduced, but also causes areas with slightly reduced or even increased precipitation to become drier (Seneviratne et al. 2012; Trenberth et al. 2013; Cook et al. 2014).

The East Asian monsoon was weakened from the late 1970s to mid-1990s, which caused a significant southward retreat of the large-scale monsoon precipitation areas in eastern China, while during the same period North China experienced a higher frequency of drought events (Huijun 2001; Zou et al. 2005; Ding et al. 2008; Dai 2013; Yu et al. 2014; Chen and Sun 2017). Although the global warming slowdown since 1998 has been highly controversial, and aroused great public interest over the past several years (Trenberth and Fasullo 2013; Tollefson 2014; Delworth et al. 2015; Fyfe et al. 2016; Yan et al. 2016; Medhaug et al. 2017; Wang et al. 2019), observations from China's mainland showed that the warming trend has slowed in northern China, particularly in northern North China and northeast China (Li et al. 2015; Sun et al. 2018). In this period, accompanied by the strengthening of the summer monsoon and the overall northward shifting of summer precipitation belt, precipitation trend switched from a decreasing trend to a significant increasing trend after 2001 in central part of North China, and the pattern of “southern flooding and northern droughts” in China has tended to be weakened, but high-temperature events in summer have become more frequent, and drought events still occur occasionally; this was especially true in the summer of 2014 when North China suffered from severe droughts (Si and Ding 2013; Ren et al. 2015; Wang and He 2015; Wang et al. 2016; Ma et al. 2018; Wang and Yuan 2018; Chen et al. 2018). How does soil moisture change under the background of precipitation increasing instead of decreasing in northern China? Answering this question would

be helpful for understanding the mechanism of regional hydrocycle process and meteorological drought.

The present study uses the Global Land Data Assimilation System (GLDAS) and ground observations to analyze the characteristics of changes in soil moisture in North China between 1961 and 2017, with a focus on the recent regional warming slowdown period of 1998–2017. The goals were to quantitatively evaluate the direct impacts of precipitation and PET on soil moisture during 1998–2017 and 1961–97, address the possible mechanism of the interperiod difference, and investigate the facts and causes of changes in soil moisture during the regional warming slowdown period in North China, aiming to provide insight into the land surface water budget and mechanism involved in drought development in this region.

2. Data and methods

a. Data

1) SURFACE METEOROLOGICAL OBSERVATIONS

The study region and the meteorological stations distribution are illustrated in Fig. 1. Through the meteorological network of the China Meteorological Administration (CMA), this study retrieved the following types of meteorological data measured daily between 1961 and 2017 at 307 stations in the study region: mean temperature, maximum temperature, minimum temperature, relative humidity, precipitation, mean wind speed at 10-m height, and sunshine duration. The data were subjected to quality control; moreover, the daily temperature data were corrected for inhomogeneity (Li et al. 2009). The rate of data missing was less than 0.02% for daily mean temperature, maximum temperature, and minimum temperature, as well as less than 0.01% for precipitation, 0.24% for mean 10-m wind speed,

0.03% for relative humidity, and 1.12% for daylight hours. All missing data were replaced by climatological means of the whole period 1961–2017.

2) ADJUSTED GLDAS-2 SOIL MOISTURE DATA (GLDAS-2-ADJ)

Because of the difficulty in observing soil moisture over the long-term period, spatiotemporally continuous observations are lacking in most regions worldwide (Robock et al. 2000). Although experimental observations have high accuracy, they lack sufficient spatial coverage at observation sites, and thus can only provide soil moisture information in a small geographical range during a specific time period. The China Agricultural Meteorology Soil Moisture Dataset (1981–2010) (V1.0) can provide the observations of soil moisture, but there were many missing data. Most stations only have observations in the warm season (May–October), and there were only 56 soil moisture stations in North China (Fig. 1). The time series of observations were discontinuous and inhomogeneous in most cases. For the study of climate change, the length of time series was not enough either, and the spatial representation was poor. Therefore, long time series and large-spatial-scale soil moisture data were usually obtained by land surface model simulation.

This study adopted the 0–10-cm soil moisture (kg m^{-2}) data from the Noah model derived by GLDAS version 2 (GLDAS-2), with a monthly temporal resolution and a $0.25^\circ \times 0.25^\circ$ spatial resolution (Rodell et al. 2004). The GLDAS-2 has two versions, GLDAS2.0 and GLDAS2.1, forced with different datasets. The main objective of GLDAS2.0 is to create more climatologically consistent datasets, which currently cover the time period 1948–2010, and that of GLDAS2.1 is to provide up-to-date global land surface model outputs, using observations based forcing. GLDAS2.1 preserves consistency of the long-term climatological data (i.e., GLDAS2.0) to the greatest extent possible, and covers from 2000 to the present. The GLDAS2.0 data well reflect the temporal–spatial characteristics of soil moisture and significantly relate to surface observations; these data are widely used in regional climate change research (Zhang et al. 2008; Mishra et al. 2014; Spennemann et al. 2015; Park et al. 2017; Jia et al. 2018; Gu et al. 2019; Jung et al. 2020), and also used in the study of drought in North China and the monitoring of soil moisture in the Qinghai–Tibet Plateau (Bi et al. 2016; Chen et al. 2020). GLDAS2.1 soil moisture showed higher temporal precision than ECMWF Reanalysis version 5 (ERA5) in northern arid areas of China (Wu et al. 2021).

To create a long-term and consistent dataset by combining GLDAS2 and GLDAS2.1, we need to correct GLDAS-2 using correction factors developed with the overlap period (2000–10). The observed soil moisture data (in %) of the China Agricultural Meteorology Soil Moisture Dataset (1981–2010) (V1.0) was used to assess the May–September 0–10-cm soil moisture data of GLDAS2.1 and GLDAS2.0 from 2001 to 2010 for their applicability in North China. First, the observations, GLDAS2.1 data, and GLDAS2.0 data were converted to the same unit of $\text{m}^3 \text{m}^{-3}$. Given the effects of the seasonal cycle of soil moisture on the assessment, this study uses the anomalies of monthly soil moisture from May to September between 2001

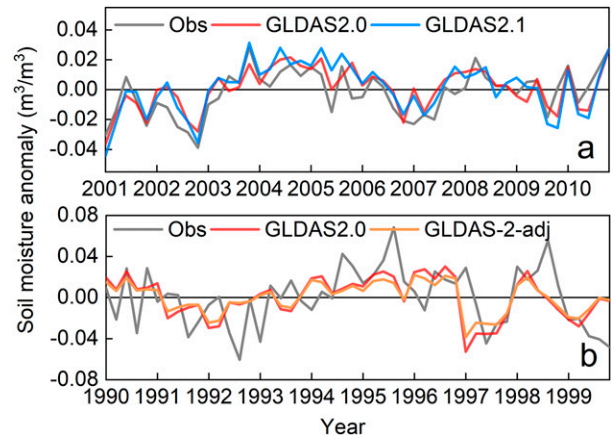


FIG. 2. (a) Comparison between the GLDAS-2 and observations (Obs) in the anomalies of monthly mean 0–10-cm soil moisture in North China from May to September between 2001 and 2010. (b) Comparison among the observations (Obs), original GLDAS2.0 (GLDAS2.0), and corrected GLDAS2.0 (GLDAS-2-adj) in the anomalies of monthly mean 0–10-cm soil moisture in North China from May to September between 1990 and 1999.

and 2010 to assess the changes in soil moisture of the GLDAS2.0, GLDAS2.1, and observations. Here, the anomalies for a given month were calculated with respect to the climatological mean soil moisture of the same month in the period 2001–10.

As shown by the anomalies of monthly soil moisture, the changes in the GLDAS2.0, GLDAS2.1, and observations were largely similar (Fig. 2a). The correlation coefficients of the GLDAS2.0 and GLDAS2.1 data with the observations were 0.78 and 0.79, respectively, with both passing the 95% confidence test, and with the new version of the GLDAS having a slightly lower root-mean-square error (RMSE), indicating that it has a similar but slightly improved simulation capability compared to the GLDAS2.0 data for soil moisture in North China. Therefore, this study adjusted GLDAS 2.0 based on GLDAS 2.1.

The difference between the GLDAS2.0 and the GLDAS2.1 data in 0–10-cm soil moisture is small, with a correlation coefficient of 0.95 and a RMSE of $0.010 \text{ m}^3 \text{ m}^{-3}$ in the period 2000–10. This study used the soil moisture data of GLDAS2.1 and GLDAS2.0 at each grid point between 2000 and 2010 to establish a univariate linear regression equation for spring [March–May (MAM)], summer [June–August (JJA)], autumn [September–November (SON)], and winter [December–February (DJF)], respectively (i.e., total samples $11 \times 3 = 33$ months). Since GLDAS2.0 differs little from GLDAS2.1, the linear regression equations all passed the 95% confidence test. The equation was used to correct the monthly soil moisture of GLDAS2.0 at each grid point between 1961 and 1999.

The observations were used to assess the May–September anomalies of monthly soil moisture data of original and corrected GLDAS2.0 from 1990 to 1999. The correlation coefficients of the original and corrected GLDAS2.0 data with the observations were 0.38 and 0.39, with both passing the 95% confidence test and a similar RMSE (0.027 and $0.026 \text{ m}^3 \text{ m}^{-3}$) (Fig. 2b). The original and corrected GLDAS2.0 data have a correlation coefficient of 0.99. This indicates that the

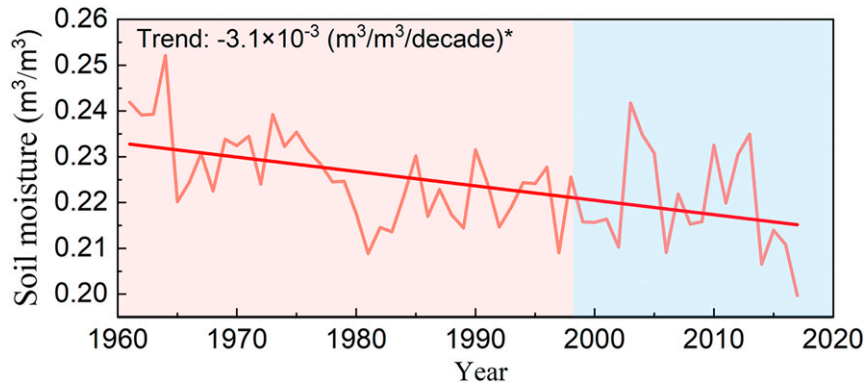


FIG. 3. Annual mean soil moisture in North China between 1961 and 2017 calculated using the GLDAS-2-adj. The asterisk represents significance of the trend at the 95% confidence interval.

corrected data have little difference from the original data and both of them are close to the observed data. The corrected time series was merged with the 2000–17 data of monthly soil moisture of GLDAS2.1 to establish a new 1961–2017 time series of 0–10-cm soil moisture at the grid points, referred to as the GLDAS-2-adj data hereafter. Based on the GLDAS-2-adj data, the time series of 0–10-cm soil moisture at the 307 stations were interpolated using kriging method.

b. Methods

1) POTENTIAL EVAPOTRANSPIRATION (PET)

According to the Penman–Monteith model (Allen et al. 1998), recommended by the United Nations (UN) Food and Agriculture Organization (FAO), meteorological observations from stations are used to calculate the PET using Eq. (1):

$$\text{PET} = \frac{0.408\Delta(R_n - G) + \gamma \frac{900}{T + 273} U(e_s - e_a)}{\Delta + \gamma(1 + 0.34U)}, \quad (1)$$

where PET is the potential evapotranspiration (mm day^{-1}), Δ is the slope of the saturation vapor pressure–temperature relationship ($\text{kPa } ^\circ\text{C}^{-1}$), R_n is the net radiation ($\text{MJ m}^{-2} \text{day}^{-1}$); G is the soil heat flux density ($\text{MJ m}^{-2} \text{day}^{-1}$), γ is the psychrometric constant ($\text{kPa } ^\circ\text{C}^{-1}$), and T is the mean daily air temperature at 2-m height ($^\circ\text{C}$). In addition, U is the wind speed at 2-m height (m s^{-1}), which is derived from the mean wind speed at 10-m height using an equation recommended by the UN FAO, e_a is the actual vapor pressure (kPa), and e_s is the saturation vapor pressure (kPa).

Equation (2) is used for calculating the net radiation (Yin et al. 2008):

$$R_n = 0.77 \left(0.2 + 0.79 \frac{n}{N} \right) R_{\text{sa}} - \sigma \left(\frac{T_{\text{max},k}^4 + T_{\text{min},k}^4}{2} \right) \times (0.56 - 0.25\sqrt{e_a}) + \left(0.9 \frac{n}{N} + 0.1 \right), \quad (2)$$

where σ is the Stefan–Boltzmann constant ($4.903 \times 10^{-9} \text{ MJ K}^{-4} \text{ m}^{-2} \text{ day}^{-1}$); $T_{\text{max},k}$ and $T_{\text{min},k}$ are the maximum

and minimum temperature (K), respectively; n is the actual sunshine duration (h), N is the maximum possible sunshine duration or sunshine hours (h), and R_{sa} is the extraterrestrial radiation ($\text{MJ m}^{-2} \text{day}^{-1}$).

The relative net radiation from soil heat flux density G is small, and can be calculated using the mean monthly temperature on a monthly scale using Eq. (3) (Allen et al. 1998):

$$G_{\text{mon},i} = 0.14(T_{\text{mon},i} - T_{\text{mon},i-1}), \quad (3)$$

where $T_{\text{mon},i}$ and $T_{\text{mon},i-1}$ are the monthly mean air temperature of months i and $i - 1$, respectively.

The saturation vapor pressure can be calculated using the saturation vapor pressure at the maximum and minimum temperatures as in Eqs. (4) and (5) (Milly and Dunne 2016):

$$e_s = \frac{e^\circ(T_{\text{max},k}) + e^\circ(T_{\text{min},k})}{2}, \quad (4)$$

$$e^\circ(T) = 0.6108 \exp\left(\frac{17.27T}{T + 237.3}\right). \quad (5)$$

2) PERCENT CONTRIBUTION OF PRECIPITATION AND PET TO CHANGES IN SOIL MOISTURE

Regression analysis was performed to quantify the effects of precipitation and PET on changes in soil moisture (Polyakov et al. 2010; Cheng and Huang 2016). First, the seasonal (or annual) scale data of precipitation, PET, and soil moisture were standardized to eliminate the difference in the orders of magnitude; second, a regression equation was established as Eq. (6):

$$\text{SM} = aX_p + bX_{\text{PET}}. \quad (6)$$

Equation (6) is a bivariate regression equation relating soil moisture to precipitation and PET, where SM is soil moisture, X_p is precipitation, and X_{PET} is PET; these are standardized variables. The terms a and b are the regression coefficients of precipitation and PET, respectively.

Using Eq. (7), the percent contribution of precipitation and PET to changes in soil moisture can be calculated, with the percent contributions of the two factors totaling 100%:

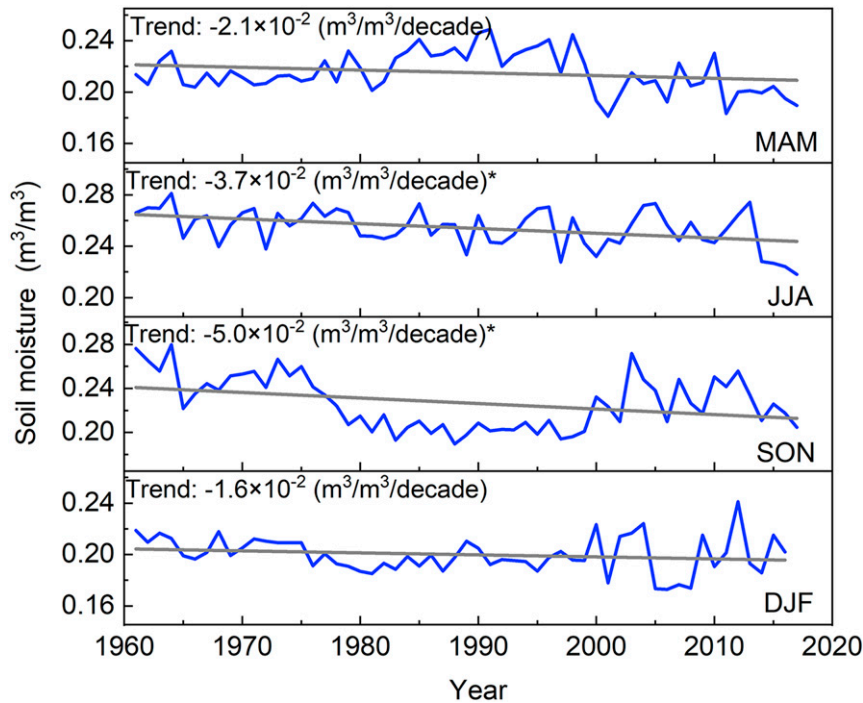


FIG. 4. Seasonal mean soil moisture in North China between 1961 and 2017 calculated using the GLDAS-2-adj. The gray straight lines represent linear trends. The asterisks represent significance of the trends at the 95% confidence interval.

$$CR = \frac{|a|}{|a| + |b|} \times 100\%. \quad (7)$$

Based on the original (none standardized) precipitation (or PET) data, a new time series of soil moisture was obtained by linear regression, which was regarded as the component of the influence of precipitation (or PET) on soil moisture, so that the contribution of precipitation (or PET) to soil moisture could be obtained by comparing with original soil moisture data (GLDAS-2-adj interpolated to the stations).

The regional means were calculated through regional gridding and area-weighted averaging. The percent anomalies of precipitation were calculated as the percent annual precipitation compared to climatological mean annual precipitation over the period 1961–2017. The linear trends and significance level were quantified and tested by the Kendall’s tau method (Kendall 1975). The mean difference of two different periods were tested for significance by the Student’s *t* test.

3. Results

a. Characteristics of changes in soil moisture

From 1961 to 2017, the annual soil moisture in North China showed a significant overall decreasing trend ($p < 0.05$) of $3.1 \times 10^{-3} \text{ m}^3 \text{ m}^{-3} \text{ decade}^{-1}$ (Fig. 3). The soil moisture was higher from the 1960s to the mid-1970s, and in particular the annual soil moisture peaked at $0.25 \text{ m}^3 \text{ m}^{-3}$ in 1964 for the past 57 years. From the end of the 1970s to the 1990s, the annual soil

moisture began to decrease over time. Although annual soil moisture was relatively high for three consecutive years, 2003–05, with the annual soil moisture in 2003 being the second highest after 1964 ($0.24 \text{ m}^3 \text{ m}^{-3}$), annual soil moisture has obviously experienced decreasing trend overall since 2003, with the annual soil moisture dropping to the 57-yr minimum of only $0.20 \text{ m}^3 \text{ m}^{-3}$ in 2017.

Soil moisture in autumn had the largest decreasing trend, at $5.0 \times 10^{-3} \text{ m}^3 \text{ m}^{-3} \text{ decade}^{-1}$, followed by summer soil moisture

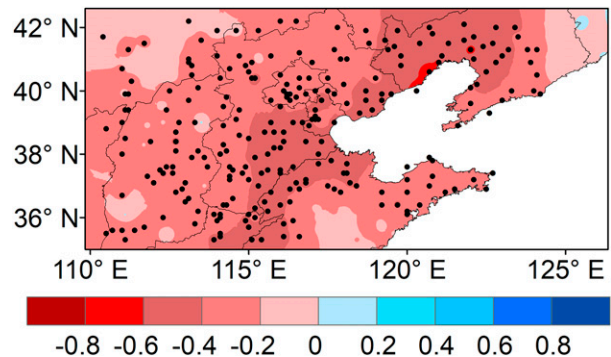


FIG. 5. Spatial distribution of the trends ($\text{m}^3 \text{ m}^{-3} \text{ decade}^{-1}$) of annual mean soil moisture in North China between 1961 and 2017 calculated using the GLDAS-2-adj, with the dark dots representing the stations with significant trends ($p < 0.05$). The values shown in legend were multiplied by 100.

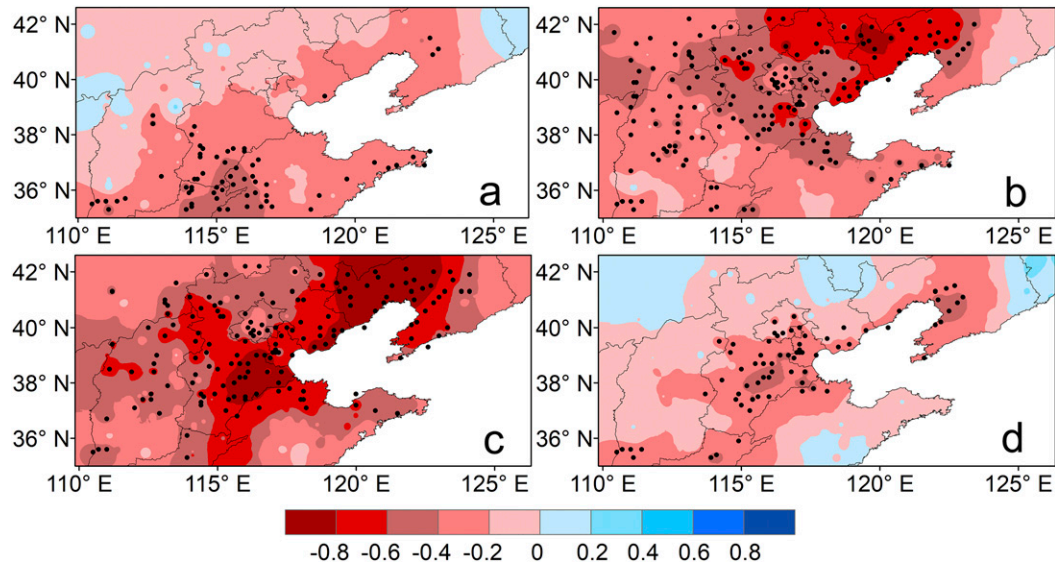


FIG. 6. Spatial distribution of the trends ($\text{m}^3 \text{m}^{-3} \text{decade}^{-1}$) of seasonal mean soil moisture in North China between 1961 and 2017 calculated using the GLDAS-2-adj, with the dark dots representing the stations with significant trends ($p < 0.05$). The values shown in legend were multiplied by 100. (a) MAM, (b) JJA, (c) SON, (d) DJF.

with a decreasing trend of $3.7 \times 10^{-3} \text{m}^3 \text{m}^{-3} \text{decade}^{-1}$, both represent significant changes ($p < 0.05$; Fig. 4). Summer soil moisture had a similar change trend to annual soil moisture, mainly because summer precipitation in North China is the largest contributor to the regional annual precipitation, and because precipitation is the most important meteorological condition affecting soil moisture. Spring and winter mean soil moisture did not change significantly over time, with decreasing at a rate of 2.1 and $1.6 \times 10^{-3} \text{m}^3 \text{m}^{-3} \text{decade}^{-1}$, respectively. Spring soil moisture was relatively high in the 1980s and 1990s but has remained relatively low since the start of the 2000s, while

autumn soil moisture exhibited an opposite trend. After 2000, the total number of years with anomalously high values of winter soil moisture increased, accompanied by an increase of the interannual variability of the soil moisture.

The spatial distribution of the soil moisture changes in North China between 1961 and 2017 is presented in Figs. 5 and 6. The 57-yr trend of annual mean soil moisture in North China was decreasing at most of stations, with the downward trend gradually becoming more pronounced from west to east and exceeding $4.0 \times 10^{-3} \text{m}^3 \text{m}^{-3} \text{decade}^{-1}$ in the eastern coastal areas (Fig. 5).

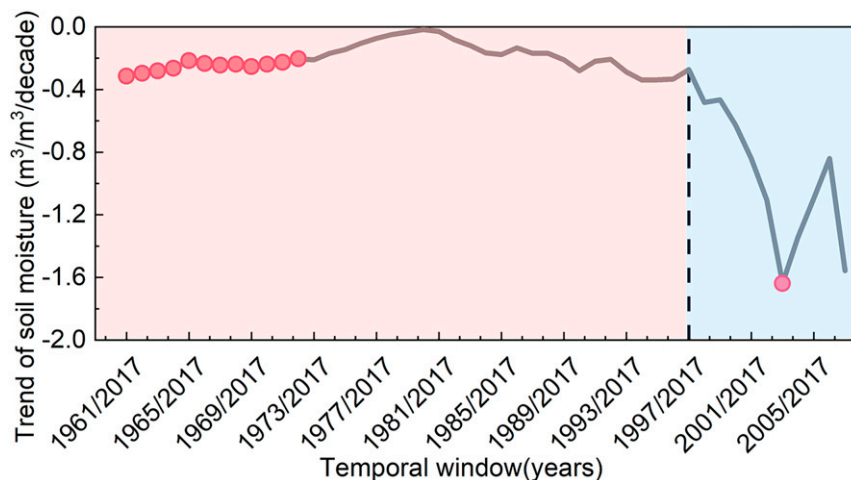


FIG. 7. Moving trends of annual mean soil moisture in North China calculated using the GLDAS-2-adj in a varied time window (the time window progressively narrows from 1961–2017 to 2007–17). The red dots represent years with significant trends ($p < 0.05$). The values shown on the y axis were multiplied by 100.

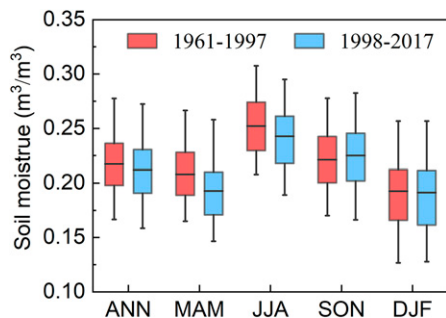


FIG. 8. Boxplots of the annual (ANN), and seasonal (MAM, JJA, SON, and DJF) mean soil moisture in North China in the periods 1961–97 and 1998–2017 calculated using the GLDAS-2-adj. The central horizontal line of the box represents the 50% quantile, the upper and lower borders of the box represent the 75% and 25% quantiles, respectively; the horizontal lines at the upper and lower ends of the vertical solid line represent the 95% and 5% quantiles, respectively.

The stations with a significantly decreasing trend of spring soil moisture were mainly distributed in the southeastern part of North China, while other areas of North China did not show a significant trend (Fig. 6a). The 57-yr trend of summer and autumn soil moisture was significantly negative at most stations in North China, and a significantly negative trend of summer soil moisture existed in a larger geographical range compared to the autumn soil moisture. Moreover, the decreasing trend of summer soil moisture at some stations in the northeastern part of North China was greater than $6.0 \times 10^{-3} \text{ m}^3 \text{ m}^{-3} \text{ decade}^{-1}$, indicating a faster drying rate than in other areas (Fig. 6b). In contrast, the stations with the most pronounced decreasing trend of autumn soil moisture were mainly located along the Bohai Sea coast in the eastern part of North China, while the areas with a decreasing trend $> 6.0 \times 10^{-3} \text{ m}^3 \text{ m}^{-3} \text{ decade}^{-1}$ were greater in number than those in summer (Fig. 6c). The stations with a significant decreasing trend of winter soil moisture were mainly located in central and northern Hebei Province, while other areas did not show a significant trend (Fig. 6d).

To further explore the characteristics of change in soil moisture during different periods, moving trend analysis was performed. The end year of the time series subjected to moving trend analysis was fixed at 2017 while the start year was 1961, after which the beginning year of time window gradually advances toward the end year while calculating the trend in each time window, namely, 1961–2017, 1962–2017, ..., 2007–17. The decreasing trend of annual soil moisture in North China became less pronounced (i.e., less negative) with a narrowing of the time window until the beginning year reached 1981, after which the decreasing trend gradually became more pronounced (i.e., more negative) (Fig. 7). The soil moisture in 2017 was the 57-yr minimum. From the end of the 1970s to the 1990s, the soil moisture was lower. In the moving trend analysis, the soil moisture of the start and end years were both dry, which led to the fact that the decreasing trend of soil moisture from 1974 to 2002 were not significant. In the regional warming slowdown

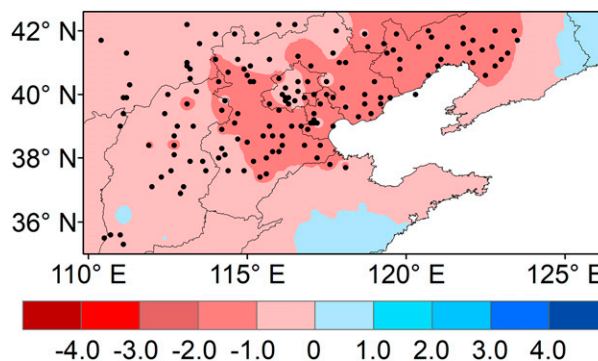


FIG. 9. Differences ($\text{m}^3 \text{ m}^{-3}$) of the climatologically annual mean soil moisture between the periods of 1998–2017 and 1961–97 in North China calculated using the GLDAS-2-adj, with the dark dots representing the stations with significant trends ($p < 0.05$). The values shown in legend were multiplied by 100.

period since 1998, the decreasing rate of annual soil moisture was faster when compared with previous periods. In particular, the decreasing trend has been most pronounced since 2003, reaching $1.6 \times 10^{-2} \text{ m}^3 \text{ m}^{-3} \text{ decade}^{-1}$ ($p < 0.05$), which were typical of short-term (less than 20 years) internal variability. The cause of the rapid drying of soil in North China since 1998 is worth exploring further.

b. Soil moisture changes during 1998–2017

Climatologically mean soil moisture in North China during 1998–2017 and 1961–97 was compared. The results show that the annual mean soil moisture was $0.2 \text{ m}^3 \text{ m}^{-3}$ between 1998 and 2017, which was lower by $7.0 \times 10^{-3} \text{ m}^3 \text{ m}^{-3}$ than that between 1961 and 1997. Moreover, the spring, summer, and winter mean soil moisture decreased from 1961–97 to 1998–2017, with the spring soil moisture showing the largest decrease of $0.02 \text{ m}^3 \text{ m}^{-3}$ ($p < 0.05$), followed by the summer soil moisture decrease ($0.01 \text{ m}^3 \text{ m}^{-3}$) ($p < 0.05$). Meanwhile, the winter soil moisture did not change much, decreasing by only $1.0 \times 10^{-3} \text{ m}^3 \text{ m}^{-3}$. Despite the trend of soil moisture was decreased in autumn from 1961 to 2017, the autumn mean soil moisture was $2.0 \times 10^{-3} \text{ m}^3 \text{ m}^{-3}$ higher during 1998–2017 than that in the 1961–97 period (Fig. 8).

The spatial distribution of the difference of the soil moisture between 1998–2017 and 1961–97 is presented in Fig. 9. From 1961–97 to 1998–2017, the annual mean soil moisture decreased by less than $0.01 \text{ m}^3 \text{ m}^{-3}$ at most stations of North China, with the stations along the Bohai Sea coast showing the most obvious decrease by up to 0.01 – $0.02 \text{ m}^3 \text{ m}^{-3}$ ($p < 0.05$). Meanwhile, a slight increase of annual mean soil moisture was observed only in the eastern part of North China near the northeast and in small areas in the south (Fig. 9).

Compared with the 1961–97 period, the spring mean soil moisture in the 1998–2017 period showed the largest decrease among the four seasons in North China; it decreased by 0.01 – $0.02 \text{ m}^3 \text{ m}^{-3}$ ($p < 0.05$) in most areas of North China and by even more than $0.02 \text{ m}^3 \text{ m}^{-3}$ in some eastern areas (Fig. 10a). Among the four seasons, the summer mean soil moisture trends had the most similar distribution to that of the annual

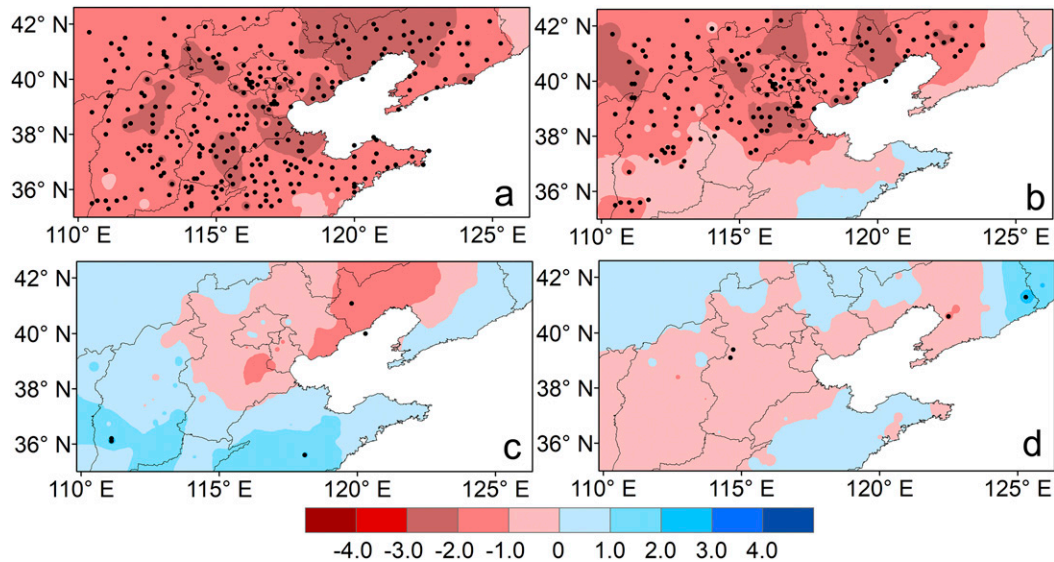


FIG. 10. Differences ($\text{m}^3 \text{m}^{-3}$) of the climatologically seasonal mean soil moisture between the periods of 1998–2017 and 1961–97 in North China calculated using the GLDAS-2-adj, with the dark dots representing the stations with significant trends ($p < 0.05$). The values shown in legend were multiplied by 100. (a) MAM, (b) JJA, (c) SON, (d) DJF.

mean soil moisture, with the southern coastal areas of North China experiencing an increase and the other areas showing a decrease; however, a decrease by $0.01\text{--}0.02 \text{m}^3 \text{m}^{-3}$ was observed in a smaller range as compared with spring (Fig. 10b). The autumn soil moisture decreased slightly in the eastern coastal areas but increased to some extent in most other areas; the areas with the largest increase were located in the southern part of North China (Fig. 10c). The winter mean soil moisture decreased in the central part of North China but increased to some extent in other areas (Fig. 10d).

c. Possible causes of the soil moisture decrease during 1998–2017

1) CHARACTERISTICS OF CHANGES IN PRECIPITATION AND PET

Precipitation was one of the main sources of soil moisture. Since 1961, the annual precipitation in North China decreased at a rate of $1.9\% \text{decade}^{-1}$ and has decreased by about 11% in 57 years overall (Fig. 11a). The 1960s and early 1970s were the periods when North China had relatively high precipitation, and in particular the highest annual precipitation over the 57 years was observed in 1964, which was higher by 47% than the climatological mean. From the 1980s to 1990s, North China received less precipitation, and lower-than-normal annual precipitation was observed in about 70% of the years, especially between 1999 and 2002 when farmers in North China suffered from severe drought for four consecutive years, with the lowest mean annual precipitation on record occurring in 1999 (Ren et al. 2015). Since 2000, precipitation gradually shifted to a period of increase, but soil moisture did not increase with the increase of precipitation in the 2000s.

For given atmospheric and radiative conditions, PET is the surface evapotranspiration rate that would occur if the soil

and vegetation were well watered (Scheff and Frierson 2014). Therefore, changes in PET have an important effect on changes in soil moisture. From 1961 to 2017, PET in North China decreased at a rate of $4.9 \text{mm yr}^{-1} \text{decade}^{-1}$ and cumulatively decreased by about 28mm yr^{-1} over the entire period (Fig. 11b). A downward trend in PET was observed until 1990s, after which the trend leveled off and PET even

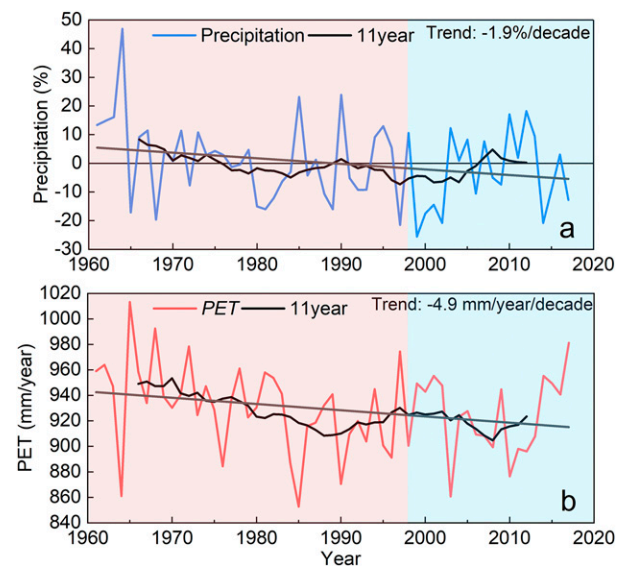


FIG. 11. Changes in percent anomalies of annual precipitation and annual PET in North China between 1961 and 2017. The black curves present the 11-yr moving means; gray straight lines represent linear trends. (a) Percent anomalies of annual precipitation and (b) annual mean PET.

TABLE 1. Trends of annual mean soil moisture (SM; $\times 10^{-3} \text{ m}^3 \text{ m}^{-3} \text{ decade}^{-1}$), precipitation (PRE; mm decade^{-1}), and potential evapotranspiration (PET; $\text{mm yr}^{-1} \text{ decade}^{-1}$) in different periods. An asterisk indicates $p < 0.05$.

Periods	SM	PRE	PET
1961–2017	−3.1*	−12.2	−4.9
1961–97	−5.5*	−25.3	−12.2*
1998–2017	−4.8	24.5	7.7

tended upward, which was consistent with the trend of annual PET in China (Ren and Guo 2006; Yin et al. 2010). Figure 9b shows that the annual PET has risen sharply since 2011, possibly experiencing the largest increase over a 10-yr period in the past 57 years.

The trends of regionally averaged soil moisture, precipitation, and PET in different periods are compared in Table 1. From 1961 to 2017, the annual mean soil moisture, precipitation, and PET all showed decreasing trends. PET may result in a slowing of the decrease in soil moisture in this period. During 1961–97, the trends of the annual mean soil moisture, precipitation and PET showed decreasing trends greater than that from 1961 to 2017. From 1998 to 2017, the annual precipitation and PET showed increasing trends, but soil moisture showed a downward trend. This suggests that increasing of PET may have resulted in the reduction of soil moisture, and it has a greater effect on soil moisture than precipitation during 1998–2017.

2) LINKS OF SOIL MOISTURE WITH PRECIPITATION AND PET

As implied above, there seemed to be a difference in the effects of precipitation and PET on soil moisture in terms of trend and interannual variability before versus after the mid-1990s. From 1961 to 2017, the correlation coefficient of annual 0–10-cm soil moisture with annual precipitation in North China was 0.81 ($p < 0.05$), and the correlation coefficient with PET was -0.39 ($p < 0.05$). However, the correlations of precipitation

and PET with soil moisture changed during the two periods of 1961–97 and 1998–2017. Between 1998 and 2017, the correlation of annual precipitation with annual mean soil moisture was weaker than that between 1961 and 1997, with the correlation coefficient decreasing from 0.83 to 0.76 (Fig. 12a). Nevertheless, the correlation coefficient of annual mean PET with annual soil moisture increased from -0.28 to -0.75 (Fig. 12b). Based on the changes in the correlation coefficient, precipitation had a stronger correlation with soil moisture than PET did for the 1961–97 period, but PET exerted an increasing impact on soil moisture during 1998–2017.

To further quantitatively compare the impacts of precipitation versus PET on soil moisture in different periods, the time series of annual precipitation and annual PET in each period (i.e., 1961–97 versus 1998–2017) were respectively multiplied by the corresponding regression coefficient of the linear regression equation to obtain two time series of soil moisture, one considered as the soil moisture component predicted by precipitation and the other by PET. Next, the time series of original soil moisture (GLDAS-2-adj), precipitation-predicted soil moisture, and the PET-predicted soil moisture were compared with each other in terms of their long-term trends in the periods of 1961–97 versus 1998–2017.

From 1961 to 1997, the original soil moisture data in North China showed a significant decreasing trend at each station, with the most pronounced trend observed along the Bohai Sea coast in the southeastern part of North China and ranging between 6.0 and $8.0 \times 10^{-3} \text{ m}^3 \text{ m}^{-3} \text{ decade}^{-1}$ (Fig. 13a). The precipitation-predicted soil moisture showed a decreasing trend at each station except for some stations in the north where a slight increasing trend was observed, and had a smaller yet similar overall trend compared with the original soil moisture data (Fig. 13c). In addition, PET showed a decreasing trend between 1961 and 1997, while the PET-predicted soil moisture showed a weak increasing trend at almost every station (Fig. 13e), indicating that the reduction of soil moisture in this period was mainly caused by the reduction of precipitation. Simultaneously, PET also declined during this period. Although the impact of PET on soil

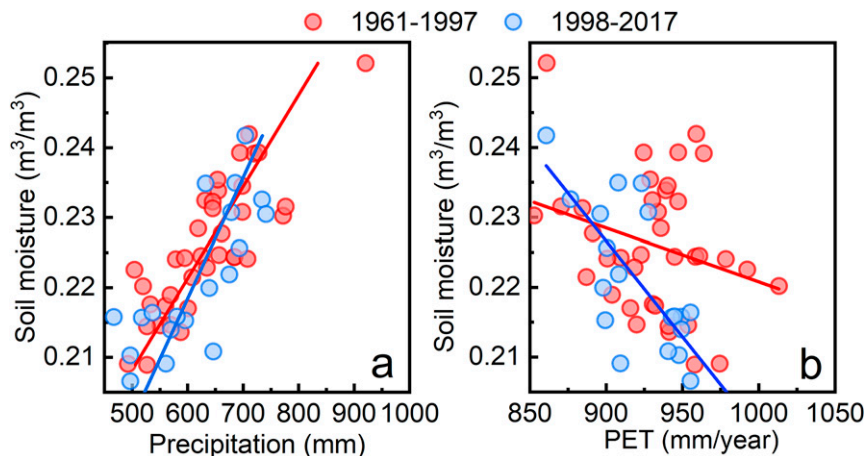


FIG. 12. Scatterplots of annual precipitation and PET vs annual mean soil moisture, in the two periods: 1961–97 and 1998–2017. (a) Precipitation and (b) PET.

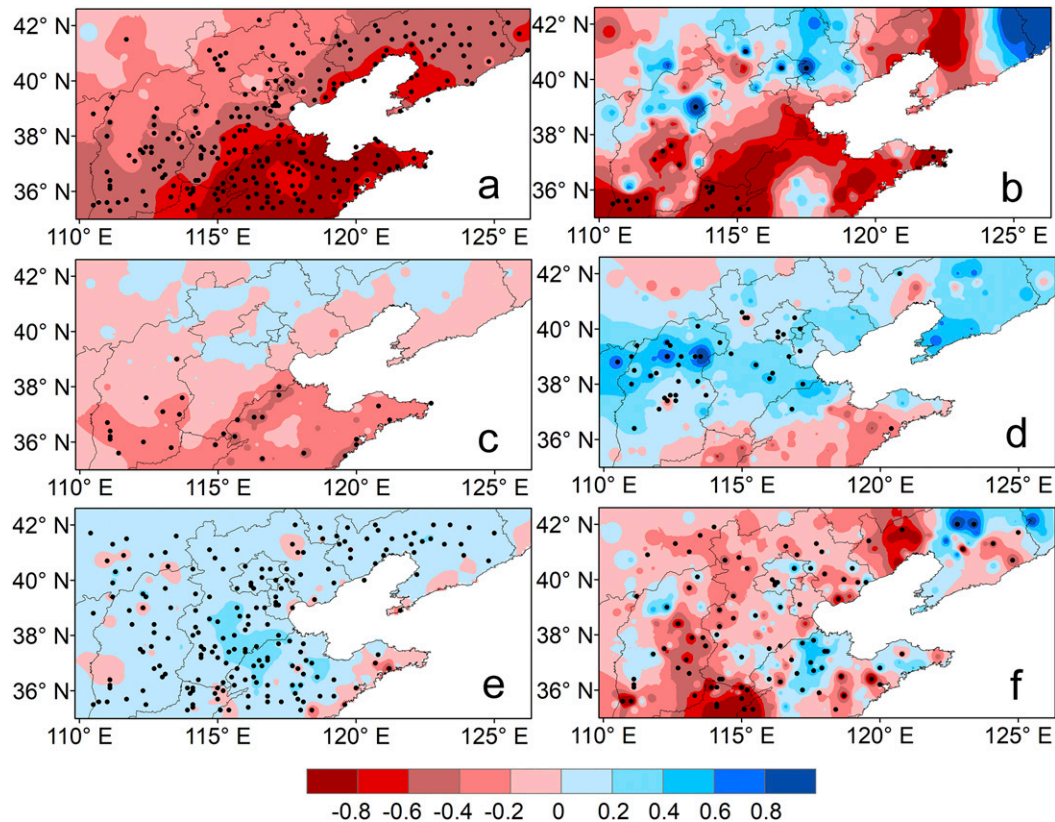


FIG. 13. Spatial distribution of the trends ($\text{m}^3 \text{m}^{-3} \text{decade}^{-1}$) of annual mean soil moisture in North China for (left) 1961–97 and (right) 1988–2017. (a),(b) Original soil moisture (GLDAS-2-adj); (c),(d) precipitation-predicted soil moisture; and (e),(f) PET-predicted soil moisture. Black dots denote the stations with significant trends ($p < 0.05$). The values shown in legend were multiplied by 100.

moisture was weaker than that of precipitation, the reduction of PET could alleviate the reduction in soil moisture to some extent.

Compared with 1961–97, the regions showing a decreasing trend in the original soil moisture was smaller in 1988–2017. In this period, soil moisture showed an increasing trend in central Inner Mongolia Province, northern Shanxi Province, northern Hebei Province, and Beijing, and the soil drying trend in other regions was also less pronounced than in 1961–97 (Fig. 13b). The precipitation-predicted soil moisture indicated an increasing trend in North China except for the southern part where a decreasing trend was observed; in particular, the most significant increase was observed in Beijing and other central areas of North China (Fig. 13d). The PET-predicted soil moisture showed a decreasing trend in North China except for northern Shandong Province and western Liaoning Province where an increasing trend was noted (Fig. 13f). These results suggest that, during 1988–2017, soil moisture increased in central Inner Mongolia Province located in the northern part of North China as well as in northern Shanxi Province, northern Hebei Province, and the Beijing area, mainly due to a gradual increase in precipitation, while soil moisture decreased in most other areas of North China, mainly because of the large-scale increase in PET.

As shown above, the impacts of precipitation and PET on soil moisture underwent changes from 1961–97 to 1988–2017. The percent contribution of precipitation and PET on soil moisture variation was used to quantitatively evaluate the effects in different periods (Fig. 14). During 1961–2017, the annual precipitation had a much higher percent contribution (86%) to soil moisture than PET did. Moreover, the summer, autumn, and winter precipitation had relatively high percentages of contribution of 80%, 82%, and 53%, respectively, while spring soil moisture was almost completely affected by PET, with a percent contribution of nearly 99%.

The percent contributions of precipitation and PET to soil moisture variability during 1961–97 were similar to those during 1961–2017 except for the winter precipitation, which had an obviously higher percent contribution (70%) during 1961–97. During 1988–2017, although the annual, spring, and autumn precipitation had higher percent contributions to soil moisture variability than the annual, spring, and autumn PET did, the percent contribution of annual PET increased by 26% compared to 1961–97. Moreover, the summer and winter PET during 1988–2017 had higher percent contributions to soil moisture variability than the summer and winter precipitation did in the same period. Although the summer PET during 1988–2017 presented an increasing trend of only $0.3 \text{ mm decade}^{-1}$, its contribution to soil

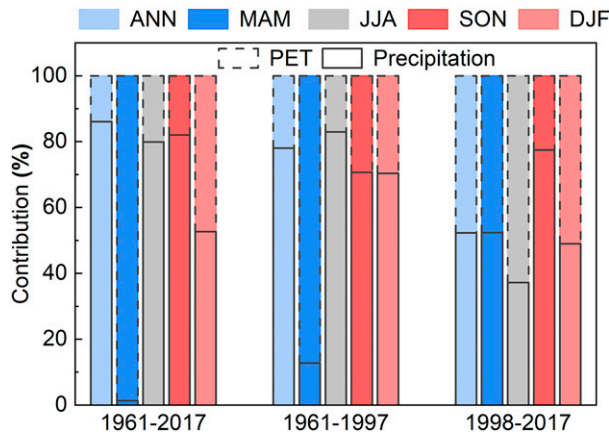


FIG. 14. Percent contributions of the annual and seasonal precipitation vs PET to the annual and seasonal soil moisture variation in different periods (%).

moisture variability increased by 45% compared to 1961–97; similarly, the percent contribution of winter PET on soil moisture variability increased by 21% from 1961–97 to 1998–2017. Also, the percent contributions of spring and autumn precipitation increased by 40% and 7%, respectively. These results show that, from 1961–97 to 1998–2017, the percent contribution of atmospheric precipitation to soil moisture variability in North China decreased while the percent contribution of PET to soil moisture increased.

4. Discussion

In this study, the characteristics of changes in soil moisture in North China during 1961–2017 are presented and the factors influencing soil moisture changes are analyzed. The effects (e.g., percent contributions) of precipitation and PET on soil moisture in the context of different climate change periods (i.e., 1961–97 versus 1998–2017) are assessed, which provides new insights along with interesting findings and understandings of soil moisture changes. In particular, the analysis results show that, from the period of 1961–97 to the period of 1998–2017, the percent contribution of atmospheric precipitation to soil moisture variability decreased while the percent contribution of PET increased.

Kong et al. (2019) proposed that soil moisture is increasing in the northeastern (semiarid and semihumid areas) and southeastern (extremely humid areas) parts of East Asia because of the warming slowdown. The results of this study, however, indicate that the increase in PET in North China during 1998–2017 enhanced the decrease in soil moisture, which offset the effect of higher precipitation since 2001 on soil moisture, thereby causing soil moisture in most areas to decrease rather than increase.

The main meteorological factors affecting the changes in PET include solar radiation, temperature, wind speed, and relative humidity. Increased temperature leads to a higher vapor pressure deficit and evaporative demand, and thus to a potential increase in evapotranspiration, possibly leading to a

further decrease in soil moisture (Seneviratne et al. 2010). X. Liu et al. (2011) proposed that the percent contribution of air temperature to PET is higher than those of solar radiation and wind speed from 1992 to 2007; as a result, the increase of PET in the 1990s should mainly be caused by a significant increase of air temperature. Although an increase in temperature would cause an increase in PET, studies have shown that, before the 1990s, most regions of China, such as North China, Northeast China, and South China, as well as large areas of many other countries such as the United States, Australia, and India, did not experience a warming-induced enhancement of PET. This phenomenon is generally attributed to the reduction of solar radiation resulting from increased cloud cover and aerosol concentration, and the reduction of near-surface wind speed resulting from various factors (Roderick and Farquhar 2002; Qiu et al. 2003; Liu et al. 2004; Guo and Ren 2005; Ren and Guo 2006; Xu et al. 2006; Rayner 2007; Roderick et al. 2007; Zheng et al. 2009; Zhao et al. 2015). Nevertheless, since 1998, although summer air temperature continued to rise in most parts of northern China, winter and spring air temperatures in general have shown a slow decreasing trend, while the annual temperature has not shown a significant trend increase (Sun et al. 2018). This may have actually been the reflection of the climate warming slowdown of northern Hemispheric mid- to high-latitude land occurred during 1998–2014, and it could be called the regional warming slowdown. However, the increasing in PET has not been slowdown since 1998. The contrast rules out the possibility that an increase of air temperature is the major cause of the reduction of soil moisture in North China since 1998.

Since the beginning of the 1990s, the decreasing trend of solar radiation in most areas across the global land has become less pronounced or even has changed to an increasing trend; this shift was described as a change from “dimming” to “brightening” (Wild et al. 2005). During this period, due to a decrease in aerosol optical thickness and an increase in atmospheric transparency, the sunshine duration and solar radiation at the land surface gradually stopped decreasing and began to stabilize, and even began to rise (Wild 2012; H. Zhang et al. 2013; Feng and Li 2018; S. Yang et al. 2018, 2019). Also, the rate of reduction in near-surface wind speed in China was also becoming smaller (Ren et al. 2005; Jiang et al. 2010; Guo et al. 2011; Lin et al. 2013). The steady increase in solar radiation and wind speed, coupled with the continued increase in land surface air temperature during summer and autumn (Sun et al. 2018), may be the main factors leading to the increase of PET, which in turn caused the continued reduction of soil moisture (Fig. 15).

The analysis of this study indicates that during 1961–97, PET contributed 22% to the annual soil moisture variation; that is, the decrease in evapotranspiration mitigated, to some extent, the degree and rate of soil moisture reduction caused by a decrease in precipitation. However, the percent contribution of PET to the annual soil moisture variation during 1998–2017 was 48%, and it was even greater than 60% in summer; that is, the enhancement of evapotranspiration largely inhibited the increasing trend of soil moisture caused by the increase of

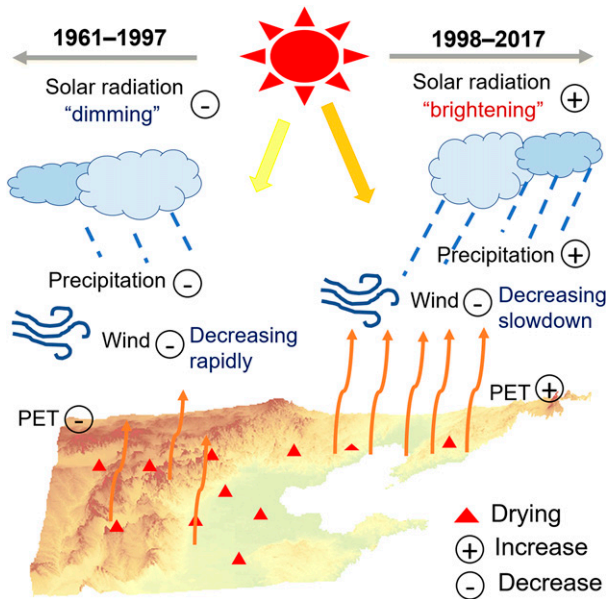


FIG. 15. Schematic plot of the effect of precipitation and PET on soil moisture during 1961–97 and 1998–2017.

precipitation and became the most important cause of the significant reduction of soil moisture since 1998.

In the two periods of 1961–97 and 1998–2017, PET contributed 87% and 99% to soil moisture variation in spring, respectively, indicating that PET plays an absolute leading role in the changes in soil moisture in spring. This may be attributed to the fact that precipitation in North China is mainly concentrated in summer and autumn, but rarely rainfalls in spring when the wind speed is the highest among all seasons and thus results in the second highest seasonal mean PET after summer. The high spring PET coupled with the low spring precipitation results in a far greater percent contribution of PET on soil moisture than that of precipitation.

In the past 20 years, the annual and summer precipitation in North China increased to some extent, and soil moisture has decreased, but drought has also slowly increased throughout the period. The reduction of the emissions of aerosols such as scattering aerosols and carbonaceous aerosols caused an increase in solar radiation in the region during the warming slowdown period (Ji et al. 2019; Liu et al. 2019), especially during the period since 2012 when the reduction in pollutant emissions has been particularly pronounced (Zhang et al. 2019). This change is related to the release and implementation of a new air pollution control policy by the Chinese government. Therefore, aerosol concentrations have decreased significantly since 2012, and the solar radiation reaching the land surface has increased, which not only accelerates evapotranspiration and soil desiccation, but also further magnifies summer warming and thereby increases PET and reduces soil moisture (Sun et al. 2019), leading to an increasing number of simultaneous occurrences of drought and high temperatures (Chen and Sun 2017; Li et al. 2019).

Therefore, PET has significantly increased since the air began to become relatively clean and is affecting soil moisture more than precipitation is, thereby reducing surface soil moisture. This in turn is increasing the risks associated with potential agricultural droughts in North China. The brightening-induced drought risk needs to be further addressed with proper coping measures.

Although the influence of PET on soil moisture has increased in recent 20 years, precipitation is still one of the main factors affecting soil moisture deficit. North China is characterized by a monsoon climate, which controls the regional precipitation variability on varied temporal scales. The East Asian summer monsoon (EASM) has been recovering since the early 1990s, although its strength is still less than in previous decades (Liu et al. 2012). A stronger EASM corresponds to more rainfall over northern China. The changes in the EASM and summer rainfall have been significantly affected by a range of natural factors including such land and oceanic thermal conditions as Eurasian snow cover, Arctic sea ice, and sea surface temperature anomalies in the Atlantic, western North Pacific, equatorial tropical Pacific, and tropical Indian Oceans (Xie et al. 2009; R. Zhang et al. 2013; Si et al. 2015; Song and Zhou 2015; Zhang 2015; Li and Wang 2018), in addition to internal variability of the coupled oceanic–atmospheric system, such as Pacific decadal oscillation (PDO), interdecadal Pacific oscillation (IPO), and Atlantic multidecadal oscillation (AMO) (Q. Yang et al. 2019). The Tibetan Plateau (TP) also played an essential role in enhancing the EASM circulation through weakened latent heating over the TP (He et al. 2019).

The output surface data of Noah model in China are not precise enough and need to be improved. The observation of soil moisture was mainly made during the warm season (May–September), the simulation ability of GLDAS2.1 and GLDAS2.0 in North China from 2001 to 2010 was evaluated for only May–September soil moisture, and no comparative evaluation was made for other seasons due to the lack of actual observations. Moreover, the influence of irrigation was not considered, which would increase the uncertainty of soil moisture simulation. Therefore, different data sources can be added and used in the future to conduct a more comprehensive research on the variation characteristics of soil moisture.

There may be mainly two additional uncertainties when measuring the contribution of precipitation and PET to soil moisture trend. First, there were other factors affecting soil moisture. Precipitation and PET can only explain parts of the variability in soil moisture, and soil moisture also had feedback to the regional precipitation and PET. Second, the process of land–atmosphere interaction was very complex. In this study, only linear regression was used to evaluate the relative contribution rates of precipitation and PET. In the future, therefore, it will be necessary to strengthen the research on the interaction of soil moisture, precipitation, PET and other factors, and also to use land surface model simulation and other methods to evaluate the relative contribution rate of precipitation and PET to soil moisture trend.

5. Conclusions

By analyzing the characteristics of soil moisture changes and their influential factors in North China between 1961 and 2017,

and particularly during 1998–2017, the following conclusions are drawn:

- 1) From 1961 to 2017, annual mean soil moisture in North China showed a significant overall decreasing trend. The decreasing trend of annual mean soil moisture at stations gradually increased from west to east, and it was most pronounced in autumn, followed by summer, while spring and winter soil moisture did not see a significant decrease.
- 2) No pause in the decrease of annual soil moisture during warming slowdown period (1998–2017) was detectable, and a decreasing trend in annual soil moisture was more pronounced than before, especially since 2003. During this period, the annual soil moisture and the spring, summer, and winter soil moisture in most areas of North China were lower than their counterparts during 1961–97, with the decrease showing spatial and seasonal differences.
- 3) The effects of precipitation and PET on soil moisture variation underwent significant changes from 1961–97 to 1998–2017. Between 1998 and 2017, the effects of PET on soil moisture gradually increased compared to the earlier period, with the percent contribution of annual PET to soil moisture variability increased by 26%; in addition, the percent contribution of summer PET increased by 45%. The increase in PET has led to a decrease of the summer and annual soil moisture.

Acknowledgments. This study is supported by the National Key R&D Program of China (2018YFA0605603), the Third Batch of Ningxia Youth Talents Supporting Program (TJGC2018043), the Ningxia Youth top talent training project, and the Natural Science Foundation of China (NSFC) (41575003).

REFERENCES

- Allen, R. G., L. S. Pereira, D. Raes, and M. Smith, 1998: Crop evapotranspiration: Guidelines for computing crop water requirements. FAO Irrigation and Drainage Paper 56, 300 pp., www.fao.org/docrep/X0490E/X0490E00.htm.
- Basso, B., R. A. Martinez-Feria, L. Rill, and J. T. Ritchie, 2021: Contrasting long-term temperature trends reveal minor changes in projected potential evapotranspiration in the US Midwest. *Nat. Commun.*, **12**, 1476, <https://doi.org/10.1038/s41467-021-21763-7>.
- Bi, H., J. Ma, W. Zheng, and J. Zeng, 2016: Comparison of soil moisture in GLDAS model simulations and in situ observations over the Tibetan Plateau. *J. Geophys. Res. Atmos.*, **121**, 2658–2678, <https://doi.org/10.1002/2015JD024131>.
- Chen, H., and J. Sun, 2017: Anthropogenic warming has caused hot droughts more frequently in China. *J. Hydrol.*, **544**, 306–318, <https://doi.org/10.1016/j.jhydrol.2016.11.044>.
- Chen, N., and Coauthors, 2020: Drought propagation in Northern China Plain: A comparative analysis of GLDAS and MERRA-2 datasets. *J. Hydrol.*, **588**, 125026, <https://doi.org/10.1016/j.jhydrol.2020.125026>.
- Chen, Y., P. Zhai, and B. Zhou, 2018: Detectable impacts of the past half-degree global warming on summertime hot extremes in China. *Geophys. Res. Lett.*, **45**, 7130–7139, <https://doi.org/10.1029/2018GL079216>.
- Cheng, S., and J. Huang, 2016: Enhanced soil moisture drying in transitional regions under a warming climate. *J. Geophys. Res. Atmos.*, **121**, 2542–2555, <https://doi.org/10.1002/2015JD024559>.
- , X. Guan, J. Huang, F. Ji, and R. Guo, 2015: Long-term trend and variability of soil moisture over East Asia. *J. Geophys. Res. Atmos.*, **120**, 8658–8670, <https://doi.org/10.1002/2015JD023206>.
- Cook, B. I., J. E. Smerdon, R. Seager, and S. Coats, 2014: Global warming and 21st century drying. *Climate Dyn.*, **43**, 2607–2627, <https://doi.org/10.1007/s00382-014-2075-y>.
- Dai, A., 2013: Increasing drought under global warming in observations and models. *Nat. Climate Change*, **3**, 52–58, <https://doi.org/10.1038/nclimate1633>.
- Delworth, T. L., F. Zeng, A. Rosati, G. A. Vecchi, and A. T. Wittenberg, 2015: A link between the hiatus in global warming and North American drought. *J. Climate*, **28**, 3834–3845, <https://doi.org/10.1175/JCLI-D-14-00616.1>.
- Ding, Y., Z. Wang, and Y. Sun, 2008: Inter-decadal variation of the summer precipitation in East China and its association with decreasing Asian summer monsoon. Part I: Observed evidences. *Int. J. Climatol.*, **28**, 1139–1161, <https://doi.org/10.1002/joc.1615>.
- Feng, H., and M. Zhang, 2015: Global land moisture trends: Drier in dry and wetter in wet over land. *Sci. Rep.*, **5**, 18018, <https://doi.org/10.1038/srep18018>.
- Feng, Y., and Y. Li, 2018: Estimated spatiotemporal variability of total, direct and diffuse solar radiation across China during 1958–2016. *Int. J. Climatol.*, **38**, 4395–4404, <https://doi.org/10.1002/joc.5676>.
- Fyfe, J. C., and Coauthors, 2016: Making sense of the early-2000s warming slowdown. *Nat. Climate Change*, **6**, 224–228, <https://doi.org/10.1038/nclimate2938>.
- Gu, X., J. Li, Y. D. Chen, D. Kong, and J. Liu, 2019: Consistency and discrepancy of global surface soil moisture changes from multiple model-based data sets against satellite observations. *J. Geophys. Res. Atmos.*, **124**, 1474–1495, <https://doi.org/10.1029/2018JD029304>.
- Guo, J., and G. Ren, 2005: Recent change of pan evaporation and possible climate factors over the Huang-Huai-Hai watershed, China (in Chinese). *Adv. Water Sci.*, **16**, 666–672.
- Guo, H., M. Xu, and Q. Hu, 2011: Changes in near-surface wind speed in China: 1969–2005. *Int. J. Climatol.*, **31**, 349–358, <https://doi.org/10.1002/joc.2091>.
- He, C., Z. Wang, T. Zhou, and T. Li, 2019: Enhanced latent heating over the Tibetan Plateau as a key to the enhanced East Asian summer monsoon circulation under a warming climate. *J. Climate*, **32**, 3373–3388, <https://doi.org/10.1175/JCLI-D-18-0427.1>.
- Huijun, W., 2001: The weakening of the Asian monsoon circulation after the end of 1970's. *Adv. Atmos. Sci.*, **18**, 376–386, <https://doi.org/10.1007/BF02919316>.
- Ji, D., and Coauthors, 2019: Impact of air pollution control measures and regional transport on carbonaceous aerosols in fine particulate matter in urban Beijing, China: Insights gained from long-term measurement. *Atmos. Chem. Phys.*, **19**, 8569–8590, <https://doi.org/10.5194/acp-19-8569-2019>.
- Jia, B., J. Liu, Z. Xie, and C. Shi, 2018: Interannual variations and trends in remotely sensed and modeled soil moisture in China. *J. Hydrometeorol.*, **19**, 831–847, <https://doi.org/10.1175/JHM-D-18-0003.1>.
- Jiang, Y., Y. Luo, Z. Zhao, and S. Tao, 2010: Changes in wind speed over China during 1956–2004. *Theor. Appl. Climatol.*, **99**, 421–430, <https://doi.org/10.1007/s00704-009-0152-7>.
- Jiao, W., L. Wang, W. K. Smith, Q. Chang, H. Wang, and P. D'Odorico, 2021: Observed increasing water constraint on

- vegetation growth over the last three decades. *Nat. Commun.*, **12**, 3777, <https://doi.org/10.1038/s41467-021-24016-9>.
- Jung, H. C., and Coauthors, 2020: Towards a soil moisture drought monitoring system for South Korea. *J. Hydrol.*, **589**, 125176, <https://doi.org/10.1016/j.jhydrol.2020.125176>.
- Jung, M., and Coauthors, 2010: Recent decline in the global land evapotranspiration trend due to limited moisture supply. *Nature*, **467**, 951–954, <https://doi.org/10.1038/nature09396>.
- Kendall, M. G., 1975: *Rank Correlation Methods*. 4th ed. Charles Griffin, 202 pp.
- Kong, X., and Coauthors, 2019: Decadal change in soil moisture over East Asia in response to a decade-long warming hiatus. *J. Geophys. Res. Atmos.*, **124**, 8619–8630, <https://doi.org/10.1029/2019JD030294>.
- Li, J., and B. Wang, 2018: Origins of the decadal predictability of East Asian land summer monsoon rainfall. *J. Climate*, **31**, 6229–6243, <https://doi.org/10.1175/JCLI-D-17-0790.1>.
- Li, Q., H. Zhang, X. Liu, J. Chen, W. Li, and P. Jones, 2009: A mainland China homogenized historical temperature dataset of 1951–2004. *Bull. Amer. Meteor. Soc.*, **90**, 1062–1065, <https://doi.org/10.1175/2009BAMS2736.1>.
- , and Coauthors, 2015: China experiencing the recent warming hiatus. *Geophys. Res. Lett.*, **42**, 889–898, <https://doi.org/10.1002/2014GL062773>.
- Li, X., Q. You, G. Ren, S. Wang, Y. Zhang, J. Yang, and G. Zheng, 2019: Concurrent droughts and hot extremes in northwest China from 1961 to 2017. *Int. J. Climatol.*, **39**, 2186–2196, <https://doi.org/10.1002/joc.5944>.
- Liepert, B., and A. Romanou, 2005: Global dimming and brightening and the water cycle. *Bull. Amer. Meteor. Soc.*, **86**, 622–623, <https://doi.org/10.1175/1520-0477-86.5.615>.
- Lin, C., K. Yang, J. Qin, and R. Fu, 2013: Observed coherent trends of surface and upper-air wind speed over China since 1960. *J. Climate*, **26**, 2891–2903, <https://doi.org/10.1175/JCLI-D-12-00093.1>.
- Liu, B., M. Xu, M. Henderson, and W. Gong, 2004: A spatial analysis of pan evaporation trends in China, 1955–2000. *J. Geophys. Res.*, **109**, D15102, <https://doi.org/10.1029/2004JD004511>.
- Liu, G., and Coauthors, 2019: Impact of the coal banning zone on visibility in the Beijing-Tianjin-Hebei region. *Sci. Total Environ.*, **692**, 402–410, <https://doi.org/10.1016/j.scitotenv.2019.07.006>.
- Liu, H., T. Zhou, Y. Zhu, and Y. Lin, 2012: The strengthening East Asia summer monsoon since the early 1990s. *Chinese Sci. Bull.*, **57**, 1553–1558, <https://doi.org/10.1007/s11434-012-4991-8>.
- Liu, Q., and Coauthors, 2011: The contributions of precipitation and soil moisture observations to the skill of soil moisture estimates in a land data assimilation system. *J. Hydrometeorol.*, **12**, 750–765, <https://doi.org/10.1175/JHM-D-10-05000.1>.
- Liu, X., Y. Luo, D. Zhang, M. Zhang, and C. Liu, 2011: Recent changes in pan-evaporation dynamics in China. *Geophys. Res. Lett.*, **38**, L13404, <https://doi.org/10.1029/2011GL047929>.
- Ma, Z., C. Fu, Q. Yang, Z. Zheng, M. Lv, M. Li, Y. Duan, and L. Chen, 2018: Drying trend in northern China and its shift during 1951–2016 (in Chinese). *Chin. J. Atmos. Sci.*, **42**, 951–961.
- McCabe, G. J., and D. M. Wolock, 2015: Increasing Northern Hemisphere water deficit. *Climatic Change*, **132**, 237–249, <https://doi.org/10.1007/s10584-015-1419-x>.
- Medhaug, I., M. B. Stolpe, E. M. Fischer, and R. Knutti, 2017: Reconciling controversies about the ‘global warming hiatus.’ *Nature*, **545**, 41–47, <https://doi.org/10.1038/nature22315>.
- Milly, P. C. D., and K. A. Dunne, 2016: Potential evapotranspiration and continental drying. *Nat. Climate Change*, **6**, 946–949, <https://doi.org/10.1038/nclimate3046>.
- Mishra, V., R. Shah, and B. Thrasher, 2014: Soil moisture droughts under the retrospective and projected climate in India. *J. Hydrometeorol.*, **15**, 2267–2292, <https://doi.org/10.1175/JHM-D-13-0177.1>.
- Orth, R., and S. I. Seneviratne, 2017: Variability of soil moisture and sea surface temperatures similarly important for warm-season land climate in the Community Earth System Model. *J. Climate*, **30**, 2141–2162, <https://doi.org/10.1175/JCLI-D-15-0567.1>.
- Park, S., S. Park, J. Im, J. Rhee, J. Shin, and J. Park, 2017: Downscaling GLDAS soil moisture data in East Asia through fusion of multi-sensors by optimizing modified regression trees. *Water*, **9**, 332, <https://doi.org/10.3390/w9050332>.
- Polyakov, I. V., V. A. Alexeev, U. S. Bhatt, E. I. Polyakova, and X. Zhang, 2010: North Atlantic warming: Patterns of long-term trend and multidecadal variability. *Climate Dyn.*, **34**, 439–457, <https://doi.org/10.1007/s00382-008-0522-3>.
- Qiu, X., C. Liu, and Y. Zeng, 2003: Changes of pan evaporation in the recent 40 years over the yellow river basin (in Chinese). *Ziran Ziyuan Xuebao*, **18**, 437–442.
- Rayner, D. P., 2007: Wind run changes: The dominant factor affecting pan evaporation trends in Australia. *J. Climate*, **20**, 3379–3394, <https://doi.org/10.1175/JCLI4181.1>.
- Ren, G., and J. Guo, 2006: Change in pan-evaporation and the influential factors over China: 1956–2000 (in Chinese). *Ziran Ziyuan Xuebao*, **21**, 31–44.
- , —, M. Xu, Z. Chu, and Q. Li, 2005: Climate changes of Mainland China over the past half century (in Chinese). *Acta Meteor. Sin.*, **63**, 942–956.
- , and Coauthors, 2015: Spatial and temporal patterns of precipitation variability over mainland China: II: Recent trends. *Shuikexue Jinzhan*, **26**, 451–465, <https://doi.org/10.14042/j.cnki.32.1309.2015.04.001>.
- Robock, A., and Coauthors, 2000: The Global Soil Moisture Data Bank. *Bull. Amer. Meteor. Soc.*, **81**, 1281–1299, [https://doi.org/10.1175/1520-0477\(2000\)081<1281:TGSMDB>2.3.CO;2](https://doi.org/10.1175/1520-0477(2000)081<1281:TGSMDB>2.3.CO;2).
- Rodell, M., and Coauthors, 2004: The Global Land Data Assimilation System. *Bull. Amer. Meteor. Soc.*, **85**, 381–394, <https://doi.org/10.1175/BAMS-85-3-381>.
- Roderick, M. L., and G. D. Farquhar, 2002: The cause of decreased pan evaporation over the past 50 years. *Science*, **298**, 1410–1411, <https://doi.org/10.1126/science.1075390-a>.
- , L. D. Rotstain, G. D. Farquhar, and M. T. Hobbins, 2007: On the attribution of changing pan evaporation. *Geophys. Res. Lett.*, **34**, L17403, <https://doi.org/10.1029/2007GL031166>.
- Samaniego, L., and Coauthors, 2018: Anthropogenic warming exacerbates European soil moisture droughts. *Nat. Climate Change*, **8**, 421–426, <https://doi.org/10.1038/s41558-018-0138-5>.
- Scheff, J., and D. M. W. Frierson, 2014: Scaling potential evapotranspiration with greenhouse warming. *J. Climate*, **27**, 1539–1558, <https://doi.org/10.1175/JCLI-D-13-00233.1>.
- Seneviratne, S. I., and Coauthors, 2010: Investigating soil moisture–climate interactions in a changing climate: A review. *Earth-Sci. Rev.*, **99**, 125–161, <https://doi.org/10.1016/j.earscirev.2010.02.004>.
- , and Coauthors, 2012: Swiss prealpine Rietholz bach research catchment and lysimeter: 32 year time series and 2003 drought event. *Water Resour. Res.*, **48**, W06526, <https://doi.org/10.1029/2011WR011749>.
- Si, D., and Y. Ding, 2013: Decadal change in the correlation pattern between the Tibetan Plateau winter snow and the East Asian summer precipitation during 1979–2011. *J. Climate*, **26**, 7622–7634, <https://doi.org/10.1175/JCLI-D-12-00587.1>.
- , Z.-Z. Hu, A. Kumar, B. Jha, P. Peng, W. Wang, and R. Han, 2015: Is the interdecadal variation of the summer rainfall over

- eastern China associated with SST? *Climate Dyn.*, **46**, 135–146, <https://doi.org/10.1007/s00382-015-2574-5>.
- Song, F., and T. Zhou, 2015: The crucial role of internal variability in modulating the decadal variation of the East Asian summer monsoon–ENSO relationship during the twentieth century. *J. Climate*, **28**, 7093–7107, <https://doi.org/10.1175/JCLI-D-14-00783.1>.
- Spennemann, P. C., J. A. Rivera, A. C. Saulo, and O. C. Penalba, 2015: A comparison of GLDAS soil moisture anomalies against standardized precipitation index and multisatellite estimations over South America. *J. Hydrometeorol.*, **16**, 158–171, <https://doi.org/10.1175/JHM-D-13-0190.1>.
- Sun, X., G. Ren, Y. Ren, Y. Fang, Y. Liu, X. Xue, and P. Zhang, 2018: A remarkable climate warming hiatus over Northeast China since 1998. *Theor. Appl. Climatol.*, **133**, 579–594, <https://doi.org/10.1007/s00704-017-2205-7>.
- , S. Li, and B. Liu, 2019: Comparative analysis of the mechanisms of intensified summer warming over Europe–West Asia and Northeast Asia since the Mid-1990s through a process-based decomposition method. *Adv. Atmos. Sci.*, **36**, 1340–1354, <https://doi.org/10.1007/s00376-019-9053-6>.
- Tollefson, J., 2014: Climate change: The case of the missing heat. *Nature*, **505**, 276–278, <https://doi.org/10.1038/505276a>.
- Trenberth, K. E., 2011: Changes in precipitation with climate change. *Climate Res.*, **47**, 123–138, <https://doi.org/10.3354/cr00953>.
- , and J. T. Fasullo, 2013: An apparent hiatus in global warming? *Earth's Future*, **1**, 19–32, <https://doi.org/10.1002/2013EF000165>.
- , A. Dai, G. van der Schrier, P. D. Jones, J. Barichivich, K. R. Briffa, and J. Sheffield, 2013: Global warming and changes in drought. *Nat. Climate Change*, **4**, 17–22, <https://doi.org/10.1038/nclimate2067>.
- Wang, H., and S. He, 2015: The north China/northeastern Asia severe summer drought in 2014. *J. Climate*, **28**, 6667–6681, <https://doi.org/10.1175/JCLI-D-15-0202.1>.
- Wang, L., and X. Yuan, 2018: Two types of flash drought and their connections with seasonal drought. *Adv. Atmos. Sci.*, **35**, 1478–1490, <https://doi.org/10.1007/s00376-018-8047-0>.
- Wang, A., D. P. Lettenmaier, and J. Sheffield, 2011: Soil moisture drought in China, 1950–2006. *J. Climate*, **24**, 3257–3271, <https://doi.org/10.1175/2011JCLI3733.1>.
- Wang, L., X. Yuan, Z. Xie, P. Wu, and Y. Li, 2016: Increasing flash droughts over China during the recent global warming hiatus. *Sci. Rep.*, **6**, 30571, <https://doi.org/10.1038/srep30571>.
- Wang, X., and Coauthors, 2019: No trends in spring and autumn phenology during the global warming hiatus. *Nat. Commun.*, **10**, 2389, <https://doi.org/10.1038/s41467-019-10235-8>.
- Wild, M., 2012: Enlightening global dimming and brightening. *Bull. Amer. Meteor. Soc.*, **93**, 27–37, <https://doi.org/10.1175/BAMS-D-11-00074.1>.
- , and Coauthors, 2005: From dimming to brightening: Decadal changes in solar radiation at Earth's surface. *Science*, **308**, 847–850, <https://doi.org/10.1126/science.1103215>.
- Wu, Z., H. Feng, H. He, J. Zhou, and Y. Zhang, 2021: Evaluation of soil moisture climatology and anomaly components derived from ERA5-land and GLDAS-2.1 in China. *Water Resour. Manage.*, **35**, 629–643, <https://doi.org/10.1007/s11269-020-02743-w>.
- Xie, S.-P., K. Hu, J. Hafner, H. Tokinaga, Y. Du, G. Huang, and T. Sampe, 2009: Indian Ocean capacitor effect on Indo–western Pacific climate during the summer following El Niño. *J. Climate*, **22**, 730–747, <https://doi.org/10.1175/2008JCLI2544.1>.
- Xu, C.-Y., L. Gong, T. Jiang, D. Chen, and V. P. Singh, 2006: Analysis of spatial distribution and temporal trend of reference evapotranspiration and pan evaporation in Changjiang (Yangtze River) catchment. *J. Hydrol.*, **327**, 81–93, <https://doi.org/10.1016/j.jhydrol.2005.11.029>.
- Yan, X.-H., and Coauthors, 2016: The global warming hiatus: Slowdown or redistribution? *Earth's Future*, **4**, 472–482, <https://doi.org/10.1002/2016EF000417>.
- Yang, Q., Z. Ma, P. Wu, N. P. Klingaman, and L. Zhang, 2019: Interdecadal seesaw of precipitation variability between North China and the southwest United States. *J. Climate*, **32**, 2951–2968, <https://doi.org/10.1175/JCLI-D-18-0082.1>.
- Yang, S., X. L. Wang, and M. Wild, 2018: Homogenization and trend analysis of the 1958–2016 in situ surface solar radiation records in China. *J. Climate*, **31**, 4529–4541, <https://doi.org/10.1175/JCLI-D-17-0891.1>.
- , —, and —, 2019: Causes of dimming and brightening in China inferred from homogenized daily clear-sky and all-sky in situ surface solar radiation records (1958–2016). *J. Climate*, **32**, 5901–5913, <https://doi.org/10.1175/JCLI-D-18-0666.1>.
- Yin, Y., S. Wu, D. Zheng, and Q. Yang, 2008: Radiation calibration of FAO56 Penman–Monteith model to estimate reference crop evapotranspiration in China. *Agric. Water Manage.*, **95**, 77–84, <https://doi.org/10.1016/j.agwat.2007.09.002>.
- , —, and E. Dai, 2010: Determining factors in potential evapotranspiration changes over China in the period 1971–2008 (in Chinese). *Chinese Sci. Bull.*, **55**, 3329–3337, <https://doi.org/10.1007/s11434-010-3289-y>.
- Yu, M., Q. Li, M. J. Hayes, M. D. Svoboda, and R. R. Heim, 2014: Are droughts becoming more frequent or severe in China based on the standardized precipitation evapotranspiration index: 1951–2010? *Int. J. Climatol.*, **34**, 545–558, <https://doi.org/10.1002/joc.3701>.
- Zhang, R., 2015: Changes in East Asian summer monsoon and summer rainfall over eastern China during recent decades. *Sci. Bull.*, **60**, 1222–1224, <https://doi.org/10.1007/s11434-015-0824-x>.
- Zhang, H., Q. Yin, T. Nakajima, N. M. Makiko, P. Lu, and J. He, 2013: Influence of changes in solar radiation on changes of surface temperature in China. *Acta Meteor. Sin.*, **27**, 87–97, <https://doi.org/10.1007/s13351-013-0109-8>.
- Zhang, J., W. C. Wang, and J. Wei, 2008: Assessing land–atmosphere coupling using soil moisture from the Global Land Data Assimilation System and observational precipitation. *J. Geophys. Res.*, **113**, D17119, <https://doi.org/10.1029/2008JD009807>.
- Zhang, Q., Z. Yang, X. Hao, and P. Yue, 2018: Conversion features of evapotranspiration responding to climate warming in transitional climate regions in northern China. *Climate Dyn.*, **52**, 3891–3903, <https://doi.org/10.1007/s00382-018-4364-3>.
- , and Coauthors, 2019: Drivers of improved PM_{2.5} air quality in China from 2013 to 2017. *Proc. Natl. Acad. Sci. USA*, **116**, 24 463–24 469, <https://doi.org/10.1073/pnas.1907956116>.
- Zhang, R., B. Wu, J. Han, and Z. Zuo, 2013: Effects on summer monsoon and rainfall change over China Duo to Eurasian snow cover and ocean thermal conditions. *Climate Change – Realities, Impacts over Ice Cap, Sea Level and Risks*, B. R. Singh, Ed., InTech, 227–250, <https://doi.org/10.5772/54831>.
- Zhao, S., H. Zhang, S. Feng, and Q. Fu, 2015: Simulating direct effects of dust aerosol on arid and semi-arid regions using an aerosol–climate coupled system. *Int. J. Climatol.*, **35**, 1858–1866, <https://doi.org/10.1002/joc.4093>.
- Zheng, H., X. Liu, C. Liu, X. Dai, and R. Zhu, 2009: Assessing contributions to panevaporation trends in Haihe River Basin, China. *J. Geophys. Res.*, **114**, D24105, <https://doi.org/10.1029/2009JD012203>.
- Zou, X., P. Zhai, and Q. Zhang, 2005: Variations in droughts over China: 1951–2003. *Geophys. Res. Lett.*, **32**, L04707, <https://doi.org/10.1029/2004GL021853>.